Seasonal Cycle of Sea Surface Temperature in the East Sea and its Dependence on Wind and Sea Ice

Kyung-Ae Park, Jong Yul Chung, and Kuh Kim

School of Earth and Environmental Sciences, Seoul National University, Seoul 151-742, Korea
(pka@eddies.snu.ac.kr, chungjy@snu.ac.kr, and kuhkim@ocean.snu.ac.kr)

Abstract: Harmonics of sea surface temperature (SST) in the East Sea and their possible causes are examined by analyzing NOAA/AVHRR data, SSM/I wind speeds, NSCAT wind vectors, and NCEP heat flux data. Detailed spatial structures of amplitudes and phases of the seasonal cycles and their contributions to the total variance of SST have quantitatively. The Subpolar front serves as a boundary between regions of high annual amplitudes (≥10°C) in the cold continental region and low amplitudes (≤10°C) in the Tsushima Warm Current region. The low phase center of annual cycle is located over a seamount at 132.2°E, 41.7°N south of Vladivostok. Semi-annual amplitudes are significantly large leaching over 20% of the annual amplitudes in the Tatarskiy Strait and along the continental shelf off Russian coast in fall and spring, but its forcings are substantially annual. We have shown that fall cooling is attributed by direct and local wind forcing, while spring cooling is remotely forced by cold waters from sea ices in the Tatarskiy Strait.

Introduction

The East Sea is a small semi-enclosed marginal sea of the northwest Pacific, but its oceanic phenomena and circulation are quite similar to those of the open ocean [Ichiye, 1984; Kim et al., 2001]. It is a unique place exposed to subtropical climate in summer to severe cold-air outbreak in winter. Understanding of seasonal variability of sea surface temperature (SST) in the East Sea is essential for the studies such as its circulation, atmospheric forcings, cold bottom water formation, the Subpolar Front, eddies and sea ice generation. Yashayaev and Zveryaev [2001] presented SST harmonics in the East Sea as a part of the Pacific Ocean, but provided their simple spatial distribution due to large spatial grids in the East Sea.

The main objectives of this study are to describe quantitatively detailed spatial structure of SST harmonics (amplitudes and phases) of the seasonal cycles (annual, semi-annual, three and four cycles/year) in the entire East Sea and to derive contribution of each cycle to the total variance of SST. We have also examined how the harmonics relate to atmospheric forcings and physical processes.

Data Processing and Analyses

Considering typical cloudiness over the East Sea, we have scheduled on NOAA/HRPT antenna system at SNU/RIO (Seoul National University/ Research Institute of Oceanography) to receive all the available passes of NOAA satellites. SST images about 4000 have processed to construct semi-monthly averaged SSTs for a period of 1990-1995. The cloud detection algorithm is optimized to the oceanic and atmospheric conditions over the East Sea [Park,1996]. The semi-monthly composites of 1.1-km SST images are re-mapped to 11 km spatial grids which is around internal Rossby deformation radius in the East Sea. We have used weekly wind speed data of Special Sensor Microwave/Imager (SSM/I) in 0.25°x0.25° grids for the same period of SST dataset. For coastal areas in the East Korean Bay of North Korea and off Vladivostok over which SSM/I has not covered, we have also utilized NSCAT (NASA Scatterometer) swath sea surface wind vectors although the NSCAT period is out of the current study period. We mainly focused on the first two cycles of semi-annual and annual frequencies in this study.

Contribution of Seasonal Cycle to Total Variance of SST

The seasonal cycle of SST in the East Sea considerably contributes to the total variance of SST by 90-98%(Fig. 1). In the mid-latitude oceans, the contribution of the seasonal cycle to the total variance of SST has been reported to exceed 80% and reach a peak by 96% in the center of subtropical [Yashayaev and Zveryaev, 2001]. Low contributions of the seasonal SST cycles in the North Pacific are attributed to the Kuroshio extension. Similarly, those in the East Sea are also apparently associated with the excursion of the TWC. Consequently, the Subpolar Front (SPF), extending along 40°N and 138°E, serves as a boundary of the variance ratios between regions of low values of the southern TWC area (90-95%) and high values of the northern continental side (≥96%).

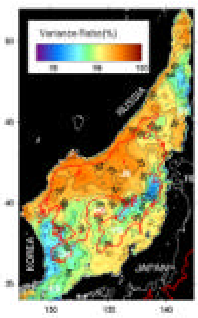

Fig.1. Contribution of the seasonal cycle to the total variance of SST(%). Abbreviations are JB, Japan Basin; YB, Yamato Rise;YR, Yamato Ridge; YB, Yamato Basin; UB, Ulleung Basin; KS, Korea Strait; SY, Soya Strait; and TS, Tsugaru Strait

Amplitudes and Variances of Annual and Semi-annual Cycles

Amplitudes of annual cycle are mostly greater than 9°C in the Japan Basin and in the northwestern part of

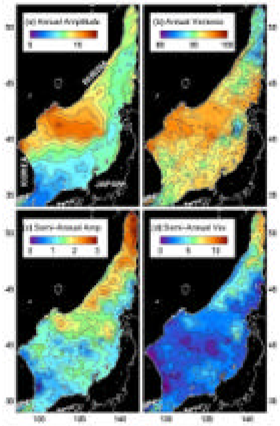

Fig. 2 (a) Annual amplitude of SST(^{o}C), (b) ratio of variance of annual cycle to total variance of SST(%), (c) semi-annual amplitude(^{o}C), and (d) ratio of variance of semi-annual cycle to the total variance of SST (%).

the East Sea, while they are small by 6^{o}C in the southern TWC part (Fig. 2a). High amplitudes greater than 11^{o}C are observed in the Peter Great Bay, 30 km south of a seamount at 132.2^{o}E, 41.7^{o}N, and in the East Korean Bay. Semi-annual amplitudes and their contribution to the total variance are quite large in these areas by greater than 2^{o}C and 8%, respectively (Fig. 2c,d). Ratio of the semi-annual amplitude to the annual amplitude ranges from 22% along the continental shelf off Russian coast to 35% in the eastern part of the Tatarskiy Strait. Semi-annual cycle of SST in the Antarctic is known to be associated with the semi-annual wave present in the atmospheric forcings of the southern hemisphere, which creates an asymmetry of SST variation with long cold period and short warm period [Van Loon, 1967; Provost et al., 1992]. What about in the East Sea? The semi-annual signal of SST in the East Sea has been poorly understood. It is of interest to investigate whether it is related to a real forcing or a subsidiary product of the harmonic fit of seasonal SSTs or not.

Phases of Annual and Semi-Annual Cycles

The phase in degrees is converted to a decimal month at which SST goes to a minimum. The East Sea is a small marginal sea, but has large north-south differences of annual phases from 1.4 to 2.2(mid February to early March), i.e. by 24 days (Fig. 3a). The earliest phase (~1.4) appears in the Tatarskiy and the Sakhaline coast. The other local minima of phases (≤1.65) are found in the Peter Great Bay, around the Flux center, the East Korea Bay, and the northeastern edge of the Japan Basin. Similar to the annual amplitude, sharp phase gradient coincides with the position of the SPF.

Annual phase depends on regional condition of air-

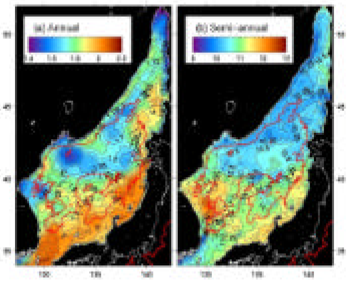

Fig. 3 Phases of (a) annual and (b) semi-annual cycles of SST in month. They are converted to a decimal month when SST goes to the minimum. Superimposed red line is 2000-m isobath of bottom topography

sea heat exchange, stratification, and mixing. It is quite interesting to understand why the phases north of the SPF are lower than those in the south. In the northern part of the East Sea, SST cooling is achieved directly by losing latent and sensible heat flux during severe cold-air outbreak in winter, whereas in its southern part the cooling is quite small due to weak wind field. In addition, continuing heat supply by the TWC delays the time of maximum SST cooling. Differences in vertical stratification and mixed layer depth (MLD) also generate large phase differences between the northern and southern part. For the same amount of net heat flux, the shallow MLD north of the SPF responds much more quickly to decrease SST than the deep southern MLD does.

A remarkable phase minimum (≤1.5) is seen as a center of circular iso-phase lines. It surprisingly coincides with the location of the seamount. Wind speeds estimated from NSCAT swath data during January 1997 are also strongest over the seamount by 13 ms^{-1} (not shown here). In order to understand why the low phase center locates over the seamount and which effect between wind and topography is more important in SST cooling during Siberian cold-air outbreak, we made simple calculation under that the assumptions of quite homogeneous water columns from the sea surface to the bottom over and adjacent to the seamount, fixed atmospheric parameters such as specific humidity, and air temperature. Temporal SST cooling is a function of net heat flux DQ as well as a depth of mixed layer D:

$$\Delta SST = \frac{\Delta Q}{r_W C_P D},$$

where r_w is water density, C_P is specific heat. The MLD is replaced by water column depth based on the assumption. Kawamura and Wu [1999] estimated the sensible and latent heat flux around the phase center as 170Wm^{-2} and 130Wm^{-2}, using NSCAT winds during January 1997. Wind speeds over the seamount are similar to those in its neighboring area (~12 ms^{-1}) with a ratio of 1/10. Thus, the net heat flux varies within 10% because wind speeds linearly contribute to net heat flux through latent and sensible heat flux changes. By contrast, the seamount depth (~1500 m) is twice as shallow as its surrounding water depth(~3000 m). Consequently, the cooling would be twice as large as those of neighboring areas. Therefore, the effect of the seamount on SST cooling is expected to be O(1) greater than the wind speed change effect from the viewpoint of its contribution to the heat flux changes. This suggests a significant role of the seamount on a surface cooling. Winds may also give an influence on SST variation through change in vertical velocity by Ekman pumping, upwelling process, and other turbulent mixing processes. The present simple calculation based on the effect of heat transfer only yields cooling by 0.12^{o}C over the seamount, which is extremely small as compared with real SST cooling at region. This implies that other processes excluding heat transfer would be more important in explaining real SST cooling.

The Tatarskiy Strait and the Primorye, with high semi-annual amplitudes over 2°C and high fractions to annual cycle, show low phases of semi-annual frequency less than 10.25(early November) as shown in Fig. 3b. Since it is a six-month period, the SST cooling also occurs six-month earlier, i.e. early May. In the western part of the Tatarskiy Strait, the phase is the lowest less than 10, i.e. SSTs begin most quickly to be damped from the annual curve in October in the entire East Sea.

Wind and Sea Ice Effects on SST Cooling

The semi-annual cycle on SST cooling in the Tatarskiy Strait and along the Russian coast occurs in fall and spring, but its forcings are substantially annual. That is, each SST cooling in November and May counts on different causes and processes. SST damping from the annual fit in spring seems to be associated with remotely-forced effects by sea-ice melting and that in fall seems to be related to direct wind forcing. The winds are the strongest during the cold-air outbreak in January, however the maximum SST cooling rate reaches not in January but in November at onset of the outbreak in the northern part of the East Sea as depicted by Park et al.[2003]. The latent heat gets to the maximum in November over most years, especially in 1991, which coincides with SST residuals from annual in early November (not shown here).

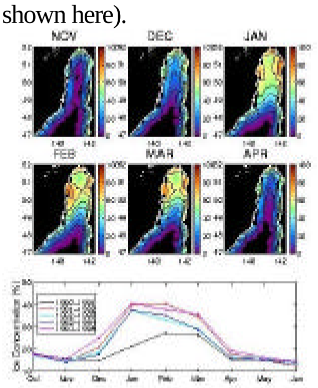

Fig. 4. Monthly distribution of sea ice concentration (%) from SSM/I from November to April and year-to-year variation of spatial mean of the sea ice concentration during winters from 1990 to 1995.

Wind field over the East Sea in May is too weak to account for the cooling and high semi-annual amplitudes. Our hypothesis is that the spring cooling in the northern part of the East Sea occurs by the advected cold waters of the southwestward-flowing Liman Current which is generated by melting of sea ices in the Tatarskiy Strait as mentioned by Martin and Kawase[1998]. The upper plots in Fig. 4 show monthly distribution of sea ice concentration from SSM/I averaged over the same period (1990-1995) of SST data set. The lower plot shows spatial mean of sea ice concentration during winter of each year. Sea ices in the Tatarskiy Strait begin to form from November, grows till January and February with maximum sea ice concentration, and melt away in April every year. The highest semi-annual amplitudes along the continental shelf off Russian coast in May have a temporal phase lag of 1-2 months with complete melting of sea ices. The lag depends on the speed of southwestward-flowing Liman Current.

Summary and Conclusion

This study presents detailed spatial structures of amplitudes, phases, variances of seasonal SST cycles in the entire East Sea covering the Tatarskiy Strait. As compared with similar latitudes in the North Pacific, the seasonal cycle in the East Sea considerably contributes to the total variance of SST by 90-98%. Since the East Sea is a distinctive place exposed to severe Siberian cold-air outbreak in winter, its wind field is crucial to determine the position and magnitude of dominant annual amplitudes and phases. Minimum of SST occurs between mid February and early March. Heat advection by the TWC plays an important role in delaying annual phases on the warm side of the SPF. Cold-air outbreak in winter decreases SST along its downwind direction and generates the lowest phase center over the seamount at 132.2°E, 41.7°N. This SST cooling by topography change at this seamount is O(1) greater than that by wind speed changes through latent and sensible heat loss. Semi-annual cycle of SST along the Primorye and in the Tatarskiy Stait is generated by two annual forcings with six-month phase lag. Cooling in November is caused by the air-sea heat transfer during the onset of cold northwesterly, while cooling in May is thought to result from cold water advection from sea-ice melting in the Tatarskiy Strait as Martin and Kawase[1998] suggested.

Acknowledgments

This research was supported by the Brain Korea 21 Project through the School of Earth and Environmental Science. SSM/I data are produced by Remote Sensing Systems and sponsored by the NASA Pathfinder Program for early Earth Observing System (EOS) products. NSCAT wind vectors are obtained from PODAAC at the NASA/JPL using DODS (Distributed Oceanographic Data System).

References

Ichiye, T., Some problems of circulation and hydrography of the Japan Sea and the Tsushima Current, 15-54. In Ocean Hydrodynamics of the Japan and East China Seas, ed. by T. Ichiye, Elsevier Oceanography Series, 39, Amsterdam, 1984.

Kawamura, H. and P. Wu, Formation mechanism of Japan Sea Proper Water in the flux center off Vladivostok, *J. Geophys. Res*, 103, C10, 21611-21622, 1998.

Kim, K, K. R. Kim, D. H. Min, Y. Volkov, J. H. Yoon, and M. Takematsu. Warming and structural changes in the East(Japan) Sea: A clue to future changes in global oceans ?, *Geophys Res. Lett*, 28(17), 3293-3296, 2001.

Martin, S. and M. Kawase, The southern flux of sea ice in the Tatarskiy Strait, Japan Sea and the generation of the Liman Current, *J. Mar. Res.*, 56, 141-155, 1998.

Provost, C., O. Garcia, and V. Garcon, Analysis of satellite sea surface temperature time series in the Brazil-Malvinas current confluence region: Dominance of the annual and semiannual periods, *J. Geophys. Res,* 97, C11, 17,841-17,858, 1992.

Van Loon, H.,The half-yearly oscillations in middle and high southern latitudes and the coreless winter, *J. Atmos., Sci.* 24, 472-486, 1967.

Yashayaev, I.M. and I. I. Zveryaev, Climate of the seasonal cycle in the North pacific and the North Atlantic Oceans, *Int. J. Climatol*, 21, 401-417, 2001.